Dynamics of structures with uncertainties: Applications to piezoelectric vibration energy harvesting

S. Adhikari[1]

[1]Chair of Aerospace Engineering, College of Engineering, Swansea University, Bay Campus, Fabian Way, Swansea, SA1 8EN, UK

Structural Mechanics and Coupled Systems Laboratory (CNAM), Paris

Swansea University

Swansea University

My research interests

- *Development* of fundamental computational methods for structural dynamics and uncertainty quantification
  A. Dynamics of complex systems
  B. Inverse problems for linear and non-linear dynamics
  C. Uncertainty quantification in computational mechanics
- *Applications* of computational mechanics to emerging multidisciplinary research areas
  D. Vibration energy harvesting / dynamics of wind turbines
  E. Computational nanomechanics

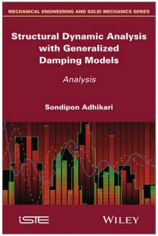

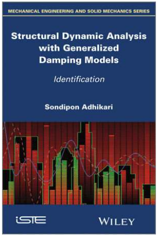

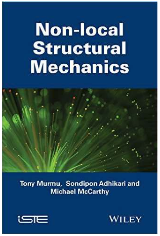

Stochastic dynamic systems - ensemble behaviour

Stochastic dynamical systems across the length-scale

Outline of the talk

Few general questions

- How does system stochasticity impact the dynamic response? Does it matter?
- What is the underlying physics?
- How can we efficiently quantify uncertainty in the dynamic response for large dynamic systems?
- What about using 'black box' type response surface methods?
- Can we use modal analysis for stochastic systems?

Stochastic SDOF systems

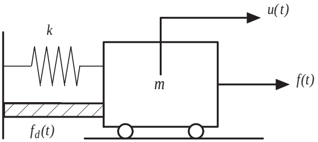

Consider a normalised single degrees of freedom system (SDOF):

$$\ddot{u}(t) + 2\zeta\omega_n\,\dot{u}(t) + \omega_n^2\,u(t) = f(t)/m \tag{1}$$

Here $\omega_n = \sqrt{k/m}$ is the natural frequency and $\xi = c/2\sqrt{km}$ is the damping ratio.

- We are interested in understanding the motion when the natural frequency of the system is perturbed in a stochastic manner.
- Stochastic perturbation can represent statistical scatter of measured values or a lack of knowledge regarding the natural frequency.

Frequency variability

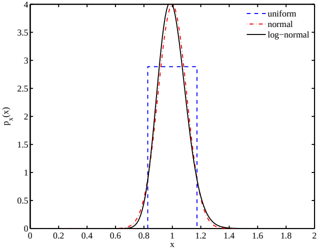

(a) Pdf: $\sigma_a = 0.1$

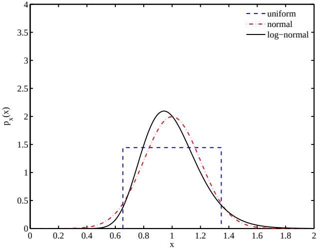

(b) Pdf: $\sigma_a = 0.2$

Figure: We assume that the mean of r is 1 and the standard deviation is σ_a.

- Suppose the natural frequency is expressed as $\omega_n^2 = \omega_{n_0}^2 r$, where ω_{n_0} is deterministic frequency and r is a random variable with a given probability distribution function.

Frequency samples

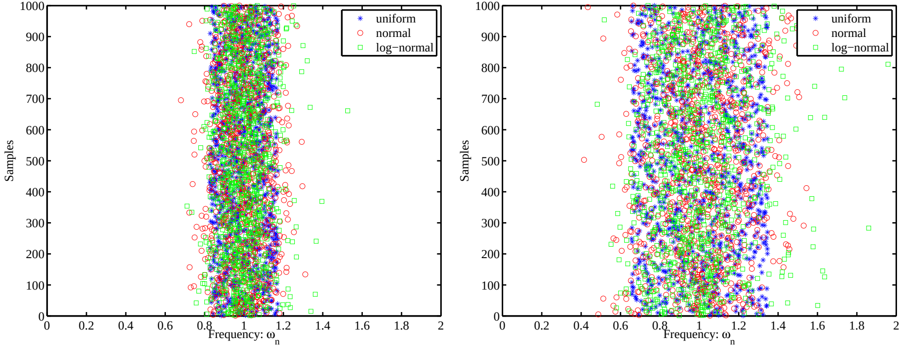

(a) Frequencies: $\sigma_a = 0.1$ (b) Frequencies: $\sigma_a = 0.2$

Figure: 1000 sample realisations of the frequencies for the three distributions

Response in the time domain

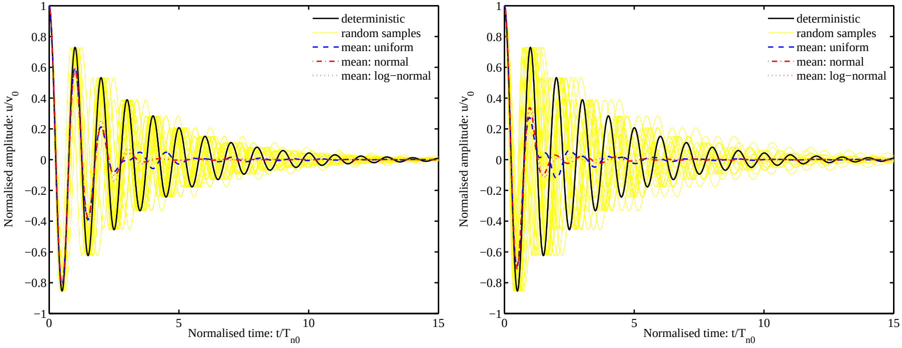

(a) Response: $\sigma_a = 0.1$ (b) Response: $\sigma_a = 0.2$

Figure: Response due to initial velocity v_0 with 5% damping

Frequency response function

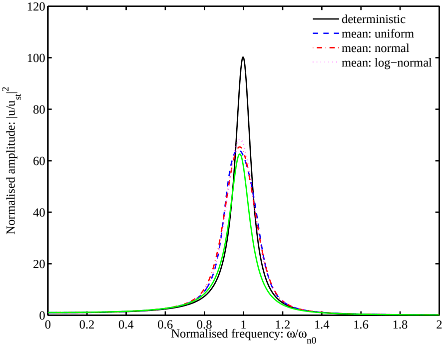

(a) Response: $\sigma_a = 0.1$

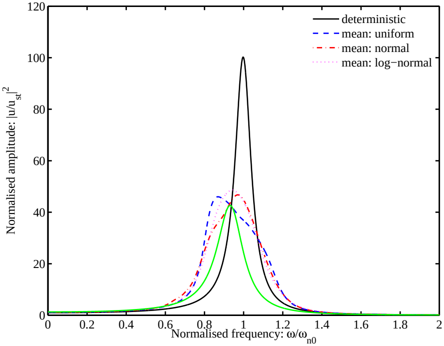

(b) Response: $\sigma_a = 0.2$

Figure: Normalised frequency response function $|u/u_{st}|^2$, where $u_{st} = f/k$

Key observations

- The mean response response is more damped compared to deterministic response.
- The higher the randomness, the higher the “effective damping”.
- The qualitative features are almost independent of the distribution the random natural frequency.
- We often use averaging to obtain more reliable experimental results - is it always true?

Assuming uniform random variable, we aim to explain some of these observations.

Equivalent damping

- Assume that the random natural frequencies are $\omega_n^2 = \omega_{n_0}^2(1+\epsilon x)$, where x has zero mean and unit standard deviation.
- The normalised harmonic response in the frequency domain

$$\frac{u(\mathrm{i}\omega)}{f/k} = \frac{k/m}{[-\omega^2 + \omega_{n_0}^2(1+\epsilon x)] + 2\mathrm{i}\xi\omega\omega_{n_0}\sqrt{1+\epsilon x}} \tag{2}$$

- Considering $\omega_{n_0} = \sqrt{k/m}$ and frequency ratio $r = \omega/\omega_{n_0}$ we have

$$\frac{u}{f/k} = \frac{1}{[(1+\epsilon x) - r^2] + 2\mathrm{i}\xi r\sqrt{1+\epsilon x}} \tag{3}$$

Equivalent damping

- The squared-amplitude of the normalised dynamic response at $\omega = \omega_{n_0}$ (that is $r = 1$) can be obtained as

$$\hat{U} = \left(\frac{|u|}{f/k}\right)^2 = \frac{1}{\epsilon^2 x^2 + 4\xi^2(1+\epsilon x)} \tag{4}$$

- Since x is zero mean unit standard deviation uniform random variable, its pdf is given by $p_x(x) = 1/2\sqrt{3}, -\sqrt{3} \leq x \leq \sqrt{3}$
- The mean is therefore

$$\begin{aligned}\mathrm{E}\left[\hat{U}\right] &= \int \frac{1}{\epsilon^2 x^2 + 4\xi^2(1+\epsilon x)} p_x(x) \mathrm{d}x \\ &= \frac{1}{4\sqrt{3}\epsilon\xi\sqrt{1-\xi^2}} \tan^{-1}\left(\frac{\sqrt{3}\epsilon}{2\xi\sqrt{1-\xi^2}} - \frac{\xi}{\sqrt{1-\xi^2}}\right) \\ &+ \frac{1}{4\sqrt{3}\epsilon\xi\sqrt{1-\xi^2}} \tan^{-1}\left(\frac{\sqrt{3}\epsilon}{2\xi\sqrt{1-\xi^2}} + \frac{\xi}{\sqrt{1-\xi^2}}\right)\end{aligned} \tag{5}$$

Equivalent damping

- Note that
$$\frac{1}{2}\left\{\tan^{-1}(a+\delta)+\tan^{-1}(a-\delta)\right\}=\tan^{-1}(a)+O(\delta^2) \tag{6}$$
- Provided there is a small δ, the mean response
$$\mathrm{E}\left[\hat{U}\right]\approx\frac{1}{2\sqrt{3}\epsilon\zeta_n\sqrt{1-\zeta_n^2}}\tan^{-1}\left(\frac{\sqrt{3}\epsilon}{2\zeta_n\sqrt{1-\zeta_n^2}}\right)+O(\zeta_n^2). \tag{7}$$
- Considering light damping (that is, $\zeta^2 \ll 1$), the validity of this approximation relies on the following inequality
$$\frac{\sqrt{3}\epsilon}{2\zeta_n}\gg\zeta_n^2 \quad \text{or} \quad \epsilon\gg\frac{2}{\sqrt{3}}\zeta_n^3. \tag{8}$$
- Since damping is usually quite small ($\zeta_n < 0.2$), the above inequality will normally hold even for systems with very small uncertainty. To give an example, for $\zeta_n = 0.2$, we get $\epsilon_{\text{min}} = 0.0092$, which is less than 0.1% randomness.
- In practice we will be interested in randomness of more than 0.1% and consequently the criteria in Eq. (8) is likely to be met.

Equivalent damping

- For small damping, the maximum deterministic amplitude at $\omega = \omega_{n_0}$ is $1/4\xi_e^2$ where ξ_e is the equivalent damping for the mean response
- Therefore, the equivalent damping for the mean response is given by

$$(2\xi_e)^2 = \frac{2\sqrt{3}\epsilon\xi}{\tan^{-1}(\sqrt{3}\epsilon/2\xi)} \tag{9}$$

- For small damping, taking the limit we can obtain[1]

$$\xi_e \approx \frac{3^{1/4}\sqrt{\epsilon}}{\sqrt{\pi}}\sqrt{\xi} \tag{10}$$

- *The equivalent damping factor of the mean system is proportional to the square root of the damping factor of the underlying baseline system*

[1] Adhikari, S. and Pascual, B., "The 'damping effect' in the dynamic response of stochastic oscillators", Probabilistic Engineering Mechanics, in press.

Equivalent frequency response function

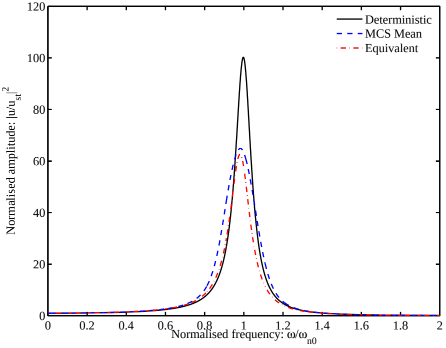

(a) Response: $\sigma_a = 0.1$

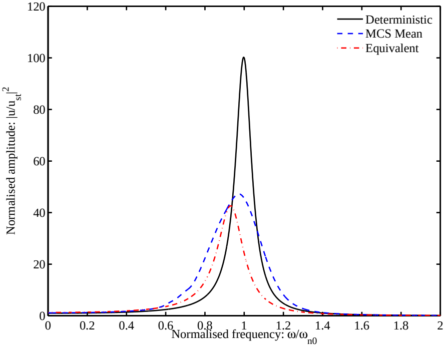

(b) Response: $\sigma_a = 0.2$

Figure: Normalised frequency response function with equivalent damping ($\xi_e = 0.05$ in the ensembles). For the two cases $\xi_e = 0.0643$ and $\xi_e = 0.0819$ respectively.

Equation for motion

- The equation for motion for stochastic linear MDOF dynamic systems:

$$\mathbf{M}(\theta)\ddot{\mathbf{u}}(\theta,t)+\mathbf{C}(\theta)\dot{\mathbf{u}}(\theta,t)+\mathbf{K}(\theta)\mathbf{u}(\theta,t)=\mathbf{f}(t) \tag{11}$$

- $\mathbf{M}(\theta)=\mathbf{M}_0+\sum_{i=1}^{p}\mu_i(\theta_i)\mathbf{M}_i \in \mathbb{R}^{n\times n}$ is the random mass matrix, $\mathbf{K}(\theta)=\mathbf{K}_0+\sum_{i=1}^{p}\nu_i(\theta_i)\mathbf{K}_i \in \mathbb{R}^{n\times n}$ is the random stiffness matrix, $\mathbf{C}(\theta)\in\mathbb{R}^{n\times n}$ as the random damping matrix, $\mathbf{u}(\theta,t)$ is the dynamic response and $\mathbf{f}(t)$ is the forcing vector.
- The mass and stiffness matrices have been expressed in terms of their deterministic components ($\mathbf{M}_0$ and $\mathbf{K}_0$) and the corresponding random contributions ($\mathbf{M}_i$ and $\mathbf{K}_i$). These can be obtained from discretising stochastic fields with a finite number of random variables ($\mu_i(\theta_i)$ and $\nu_i(\theta_i)$) and their corresponding spatial basis functions.
- Proportional damping model is considered for which $\mathbf{C}(\theta)=\zeta_1\mathbf{M}(\theta)+\zeta_2\mathbf{K}(\theta)$, where ζ_1 and ζ_2 are scalars.

Frequency domain representation

- For the harmonic analysis of the structural system, taking the Fourier transform
$$\left[-\omega^2\mathbf{M}(\theta) + i\omega\mathbf{C}(\theta) + \mathbf{K}(\theta)\right]\mathbf{u}(\omega,\theta) = \mathbf{f}(\omega) \tag{12}$$
where $\mathbf{u}(\omega,\theta) \in \mathbb{C}^n$ is the complex frequency domain system response amplitude, $\mathbf{f}(\omega)$ is the amplitude of the harmonic force.
- For convenience we group the random variables associated with the mass and stiffness matrices as

$$\xi_i(\theta) = \mu_i(\theta) \quad \text{and} \quad \xi_{j+p_1}(\theta) = \nu_j(\theta) \quad \begin{array}{ll} \text{for} & i = 1, 2, \ldots, p_1 \\ \text{and} & j = 1, 2, \ldots, p_2 \end{array}$$

Frequency domain representation

- Using $M = p_1 + p_2$ which we have

$$\left(\mathbf{A}_0(\omega) + \sum_{i=1}^{M} \xi_i(\theta)\mathbf{A}_i(\omega)\right)\mathbf{u}(\omega,\theta) = \mathbf{f}(\omega) \tag{13}$$

  where $\mathbf{A}_0$ and $\mathbf{A}_i \in \mathbb{C}^{n\times n}$ represent the complex deterministic and stochastic parts respectively of the mass, the stiffness and the damping matrices ensemble.

- For the case of proportional damping the matrices $\mathbf{A}_0$ and $\mathbf{A}_i$ can be written as

$$\mathbf{A}_0(\omega) = \left[-\omega^2 + i\omega\zeta_1\right]\mathbf{M}_0 + \left[i\omega\zeta_2 + 1\right]\mathbf{K}_0, \tag{14}$$

$$\mathbf{A}_i(\omega) = \left[-\omega^2 + i\omega\zeta_1\right]\mathbf{M}_i \quad \text{for} \quad i = 1, 2, \ldots, p_1 \tag{15}$$

$$\text{and} \quad \mathbf{A}_{j+p_1}(\omega) = \left[i\omega\zeta_2 + 1\right]\mathbf{K}_j \quad \text{for} \quad j = 1, 2, \ldots, p_2\,.$$

Possibilities of solution types

The dynamic response $\mathbf{u}(\omega, \theta) \in \mathbb{C}^n$ is governed by

$$\left[-\omega^2\mathbf{M}(\xi(\theta)) + i\omega\mathbf{C}(\xi(\theta)) + \mathbf{K}(\xi(\theta))\right]\mathbf{u}(\omega, \theta) = \mathbf{f}(\omega).$$

Some possibilities for the solutions are

$$\begin{aligned}
\mathbf{u}(\omega, \theta) &= \sum_{k=1}^{P_1} H_k(\xi(\theta))\mathbf{u}_k(\omega) \qquad \text{(PCE)}\\
\text{or} \quad &= \sum_{k=1}^{P_2} H_k(\omega))\mathbf{u}_k(\xi(\theta))\\
\text{or} \quad &= \sum_{k=1}^{P_3} a_k(\omega)H_k(\xi(\theta))\mathbf{u}_k\\
\text{or} \quad &= \sum_{k=1}^{P_4} H_k(\omega, \xi(\theta))\mathbf{u}_k \qquad \ldots \text{etc.}
\end{aligned} \tag{16}$$

Deterministic classical modal analysis?

For a deterministic system, the response vector $\mathbf{u}(\omega)$ can be expressed as

$$\begin{aligned}\mathbf{u}(\omega) &= \sum_{k=1}^{P} \Gamma_k(\omega)\mathbf{u}_k \\ \text{where} \quad \Gamma_k(\omega) &= \frac{\phi_k^T \mathbf{f}}{-\omega^2 + 2\mathrm{i}\zeta_k\omega_k\omega + \omega_k^2} \\ \mathbf{u}_k &= \phi_k \quad \text{and} \quad P \leq n \ (\text{number of dominant modes})\end{aligned} \tag{17}$$

Can we extend this idea to stochastic systems?

Projection in the modal space

There exist a finite set of complex frequency dependent functions $\Gamma_k(\omega, \xi(\theta))$ and a complete basis $\phi_k \in \mathbb{R}^n$ for $k = 1, 2, \ldots, n$ such that the solution of the discretized stochastic finite element equation (11) can be expiressed by the series

$$\hat{\mathbf{u}}(\omega, \theta) = \sum_{k=1}^{n} \Gamma_k(\omega, \xi(\theta))\phi_k \tag{18}$$

Outline of the derivation: In the first step a complete basis is generated with the eigenvectors $\phi_k \in \mathbb{R}^n$ of the generalized eigenvalue problem

$$\mathbf{K}_0\phi_k = \lambda_{0_k}\mathbf{M}_0\phi_k; \quad k = 1, 2, \ldots n \tag{19}$$

Projection in the modal space

- We define the matrix of eigenvalues and eigenvectors

$$\boldsymbol{\lambda}_0 = \mathrm{diag}\left[\lambda_{0_1}, \lambda_{0_2}, \ldots, \lambda_{0_n}\right] \in \mathbb{R}^{n\times n}; \boldsymbol{\Phi} = \left[\boldsymbol{\phi}_1, \boldsymbol{\phi}_2, \ldots, \boldsymbol{\phi}_n\right] \in \mathbb{R}^{n\times n} \tag{20}$$

  Eigenvalues are ordered in the ascending order: $\lambda_{0_1} < \lambda_{0_2} < \ldots < \lambda_{0_n}$.
- We use the orthogonality property of the modal matrix $\boldsymbol{\Phi}$ as

$$\boldsymbol{\Phi}^T \mathbf{K}_0 \boldsymbol{\Phi} = \boldsymbol{\lambda}_0, \quad \text{and} \quad \boldsymbol{\Phi}^T \mathbf{M}_0 \boldsymbol{\Phi} = \mathbf{I} \tag{21}$$

- Using these we have

$$\begin{aligned} \boldsymbol{\Phi}^T \mathbf{A}_0 \boldsymbol{\Phi} &= \boldsymbol{\Phi}^T \left([-\omega^2 + i\omega\zeta_1]\mathbf{M}_0 + [i\omega\zeta_2 + 1]\mathbf{K}_0 \right) \boldsymbol{\Phi} \\ &= \left(-\omega^2 + i\omega\zeta_1\right)\mathbf{I} + \left(i\omega\zeta_2 + 1\right)\boldsymbol{\lambda}_0 \end{aligned} \tag{22}$$

  This gives $\boldsymbol{\Phi}^T \mathbf{A}_0 \boldsymbol{\Phi} = \boldsymbol{\Lambda}_0$ and $\mathbf{A}_0 = \boldsymbol{\Phi}^{-T} \boldsymbol{\Lambda}_0 \boldsymbol{\Phi}^{-1}$, where $\boldsymbol{\Lambda}_0 = \left(-\omega^2 + i\omega\zeta_1\right)\mathbf{I} + \left(i\omega\zeta_2 + 1\right)\boldsymbol{\lambda}_0$ and $\mathbf{I}$ is the identity matrix.

Projection in the modal space

- Hence, $\boldsymbol{\Lambda}_0$ can also be written as

$$\boldsymbol{\Lambda}_0 = \mathrm{diag}\left[\lambda_{0_1}, \lambda_{0_2}, \ldots, \lambda_{0_n}\right] \in \mathbb{C}^{n\times n} \tag{23}$$

where $\lambda_{0_j} = \left(-\omega^2 + i\omega\zeta_1\right) + \left(i\omega\zeta_2 + 1\right)\lambda_j$ and λ_j is as defined in Eqn. (20). We also introduce the transformations

$$\widetilde{\mathbf{A}}_i = \boldsymbol{\Phi}^T \mathbf{A}_i \boldsymbol{\Phi} \in \mathbb{C}^{n\times n}; i = 0, 1, 2, \ldots, M. \tag{24}$$

Note that $\widetilde{\mathbf{A}}_0 = \boldsymbol{\Lambda}_0$ is a diagonal matrix and

$$\mathbf{A}_i = \boldsymbol{\Phi}^{-T} \widetilde{\mathbf{A}}_i \boldsymbol{\Phi}^{-1} \in \mathbb{C}^{n\times n}; i = 1, 2, \ldots, M. \tag{25}$$

Projection in the modal space

Suppose the solution of Eq. (11) is given by

$$\hat{\mathbf{u}}(\omega,\theta) = \left[\mathbf{A}_0(\omega) + \sum_{i=1}^{M} \xi_i(\theta) \mathbf{A}_i(\omega) \right]^{-1} \mathbf{f}(\omega) \tag{26}$$

Using Eqs. (20)–(25) and the mass and stiffness orthogonality of $\mathbf{\Phi}$ one has

$$\begin{aligned} \hat{\mathbf{u}}(\omega,\theta) &= \left[\mathbf{\Phi}^{-T} \mathbf{\Lambda}_0(\omega) \mathbf{\Phi}^{-1} + \sum_{i=1}^{M} \xi_i(\theta) \mathbf{\Phi}^{-T} \widetilde{\mathbf{A}}_i(\omega) \mathbf{\Phi}^{-1} \right]^{-1} \mathbf{f}(\omega) \\ \Rightarrow \quad \hat{\mathbf{u}}(\omega,\theta) &= \mathbf{\Phi} \underbrace{\left[\mathbf{\Lambda}_0(\omega) + \sum_{i=1}^{M} \xi_i(\theta) \widetilde{\mathbf{A}}_i(\omega) \right]^{-1}}_{\mathbf{\Psi}(\omega, \boldsymbol{\xi}(\theta))} \mathbf{\Phi}^{-T} \mathbf{f}(\omega) \end{aligned} \tag{27}$$

$$\text{where} \qquad \boldsymbol{\xi}(\theta) = \left\{ \xi_1(\theta), \xi_2(\theta), \ldots, \xi_M(\theta) \right\}^T.$$

Projection in the modal space

Now we separate the diagonal and off-diagonal terms of the $\widetilde{\mathbf{A}}_i$ matrices as

$$\widetilde{\mathbf{A}}_i = \mathbf{\Lambda}_i + \mathbf{\Delta}_i, \quad i = 1, 2, \ldots, M \tag{28}$$

Here the diagonal matrix

$$\mathbf{\Lambda}_i = \mathrm{diag}\left[\widetilde{\mathbf{A}}\right] = \mathrm{diag}\left[\lambda_{i_1}, \lambda_{i_2}, \ldots, \lambda_{i_n}\right] \in \mathbb{R}^{n \times n} \tag{29}$$

and $\mathbf{\Delta}_i = \widetilde{\mathbf{A}}_i - \mathbf{\Lambda}_i$ is an off-diagonal only matrix.

$$\mathbf{\Psi}\left(\omega, \boldsymbol{\xi}(\theta)\right) = \left[\underbrace{\mathbf{\Lambda}_0(\omega) + \sum_{i=1}^{M} \xi_i(\theta)\mathbf{\Lambda}_i(\omega)}_{\mathbf{\Lambda}(\omega,\boldsymbol{\xi}(\theta))} + \underbrace{\sum_{i=1}^{M} \xi_i(\theta)\mathbf{\Delta}_i(\omega)}_{\mathbf{\Delta}(\omega,\boldsymbol{\xi}(\theta))}\right]^{-1} \tag{30}$$

where $\mathbf{\Lambda}\left(\omega, \boldsymbol{\xi}(\theta)\right) \in \mathbb{R}^{n \times n}$ is a diagonal matrix and $\mathbf{\Delta}\left(\omega, \boldsymbol{\xi}(\theta)\right)$ is an off-diagonal only matrix.

Projection in the modal space

We rewrite Eq. (30) as

$$\mathbf{\Psi}\left(\omega, \boldsymbol{\xi}(\theta)\right) = \left[\mathbf{\Lambda}\left(\omega, \boldsymbol{\xi}(\theta)\right)\left[\mathbf{I}_n + \mathbf{\Lambda}^{-1}\left(\omega, \boldsymbol{\xi}(\theta)\right)\mathbf{\Delta}\left(\omega, \boldsymbol{\xi}(\theta)\right)\right]\right]^{-1} \tag{31}$$

The above expression can be represented using a Neumann type of matrix series as

$$\mathbf{\Psi}\left(\omega, \boldsymbol{\xi}(\theta)\right) = \sum_{s=0}^{\infty}(-1)^s\left[\mathbf{\Lambda}^{-1}\left(\omega, \boldsymbol{\xi}(\theta)\right)\mathbf{\Delta}\left(\omega, \boldsymbol{\xi}(\theta)\right)\right]^s\mathbf{\Lambda}^{-1}\left(\omega, \boldsymbol{\xi}(\theta)\right) \tag{32}$$

Projection in the modal space

Taking an arbitrary r-th element of $\hat{\mathbf{u}}(\omega,\theta)$, Eq. (27) can be rearranged to have

$$\hat{u}_r(\omega,\theta) = \sum_{k=1}^{n} \Phi_{rk} \left(\sum_{j=1}^{n} \Psi_{kj}\left(\omega, \boldsymbol{\xi}(\theta)\right) \left(\phi_j^T \mathbf{f}(\omega) \right) \right) \tag{33}$$

Defining

$$\Gamma_k\left(\omega, \boldsymbol{\xi}(\theta)\right) = \sum_{j=1}^{n} \Psi_{kj}\left(\omega, \boldsymbol{\xi}(\theta)\right) \left(\phi_j^T \mathbf{f}(\omega) \right) \tag{34}$$

and collecting all the elements in Eq. (33) for $r = 1, 2, \ldots, n$ one has[2]

$$\hat{\mathbf{u}}(\omega,\theta) = \sum_{k=1}^{n} \Gamma_k\left(\omega, \boldsymbol{\xi}(\theta)\right) \phi_k \tag{35}$$

[2] Kundu, A. and Adhikari, S., "Dynamic analysis of stochastic structural systems using frequency adaptive spectral functions", Probabilistic Engineering Mechanics, 39[1] (2015), pp. 23-38.

Spectral functions

Definition

The functions $\Gamma_k(\omega, \boldsymbol{\xi}(\theta)), k = 1, 2, \ldots n$ *are the* *frequency-adaptive spectral functions* *as they are expressed in terms of the spectral properties of the coefficient matrices at each frequency of the governing discretized equation.*

- Each of the spectral functions $\Gamma_k(\omega, \boldsymbol{\xi}(\theta))$ contain infinite number of terms and they are highly nonlinear functions of the random variables $\xi_i(\theta)$.
- For computational purposes, it is necessary to truncate the series after certain number of terms.
- Different order of spectral functions can be obtained by using truncation in the expression of $\Gamma_k(\omega, \boldsymbol{\xi}(\theta))$

First-order and second order spectral functions

Definition

The different order of spectral functions $\Gamma_k^{(1)}(\omega, \boldsymbol{\xi}(\theta)), k = 1, 2, \ldots, n$ are obtained by retaining as many terms in the series expansion in Eqn. (32).

Retaining one and two terms in (32) we have

$$\boldsymbol{\Psi}^{(1)}(\omega, \boldsymbol{\xi}(\theta)) = \boldsymbol{\Lambda}^{-1}(\omega, \boldsymbol{\xi}(\theta)) \tag{36}$$

$$\boldsymbol{\Psi}^{(2)}(\omega, \boldsymbol{\xi}(\theta)) = \boldsymbol{\Lambda}^{-1}(\omega, \boldsymbol{\xi}(\theta)) - \boldsymbol{\Lambda}^{-1}(\omega, \boldsymbol{\xi}(\theta))\,\boldsymbol{\Delta}(\omega, \boldsymbol{\xi}(\theta))\,\boldsymbol{\Lambda}^{-1}(\omega, \boldsymbol{\xi}(\theta)) \tag{37}$$

which are the first and second order spectral functions respectively.

- From these we find $\Gamma_k^{(1)}(\omega, \boldsymbol{\xi}(\theta)) = \sum_{j=1}^{n} \Psi_{kj}^{(1)}(\omega, \boldsymbol{\xi}(\theta)) \left(\boldsymbol{\phi}_j^T \mathbf{f}(\omega)\right)$ are non-Gaussian random variables even if $\xi_i(\theta)$ are Gaussian random variables.

Nature of the spectral functions

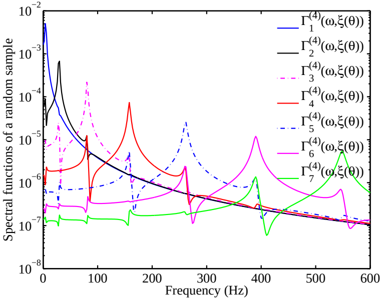

(a) Spectral functions for $\sigma_a = 0.1$.

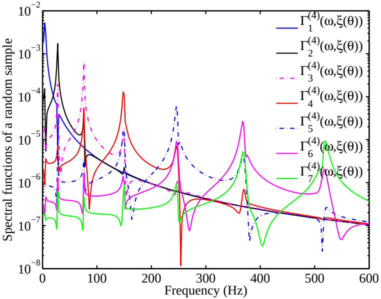

(b) Spectral functions for $\sigma_a = 0.2$.

The amplitude of first seven spectral functions of order 4 for a particular random sample under applied force. The spectral functions are obtained for two different standard deviation levels of the underlying random field: $\sigma_a = \{0.10, 0.20\}$.

Summary of the basis functions (frequency-adaptive spectral functions)

The basis functions are:

1. not polynomials in $\xi_i(\theta)$ but ratio of polynomials.
2. independent of the nature of the random variables (i.e. applicable to Gaussian, non-Gaussian or even mixed random variables).
3. not general but specific to a problem as it utilizes the eigenvalues and eigenvectors of the system matrices.
4. such that truncation error depends on the off-diagonal terms of the matrix $\mathbf{\Delta}(\omega, \boldsymbol{\xi}(\theta))$.
5. showing 'peaks' when ω is near to the system natural frequencies

Next we use these frequency-adaptive spectral functions as trial functions within a Galerkin error minimization scheme.

The Galerkin approach

One can obtain constants $c_k \in \mathbb{C}$ such that the error in the following representation

$$\hat{\mathbf{u}}(\omega, \theta) = \sum_{k=1}^{n} c_k(\omega) \widehat{\Gamma}_k(\omega, \boldsymbol{\xi}(\theta)) \phi_k \tag{38}$$

can be minimised in the least-square sense. It can be shown that the vector $\mathbf{c} = \{c_1, c_2, \ldots, c_n\}^T$ satisfies the $n \times n$ complex algebraic equations $\mathbf{S}(\omega)\, \mathbf{c}(\omega) = \mathbf{b}(\omega)$ with

$$S_{jk} = \sum_{i=0}^{M} \widetilde{A}_{i_{jk}} D_{ijk}; \quad \forall\ j, k = 1, 2, \ldots, n; \widetilde{A}_{i_{jk}} = \phi_j^T \mathbf{A}_i \phi_k, \tag{39}$$

$$D_{ijk} = \mathrm{E}\left[\xi_i(\theta) \widehat{\Gamma}_k(\omega, \boldsymbol{\xi}(\theta))\right], b_j = \mathrm{E}\left[\phi_j^T \mathbf{f}(\omega)\right]. \tag{40}$$

The Galerkin approach

- The error vector can be obtained as

$$\varepsilon(\omega,\theta) = \left(\sum_{i=0}^{M} \mathbf{A}_i(\omega)\xi_i(\theta)\right)\left(\sum_{k=1}^{n} c_k \widehat{\Gamma}_k(\omega, \boldsymbol{\xi}(\theta))\phi_k\right) - \mathbf{f}(\omega) \in \mathbb{C}^{N\times N} \quad (41)$$

  The solution is viewed as a projection where $\phi_k \in \mathbb{R}^n$ are the basis functions and c_k are the unknown constants to be determined. This is done for each frequency step.

- The coefficients c_k are evaluated using the Galerkin approach so that the error is made orthogonal to the basis functions, that is, mathematically

$$\varepsilon(\omega,\theta) \perp \phi_j \Rrightarrow \left\langle \phi_j, \varepsilon(\omega,\theta)\right\rangle = 0 \, \forall \, j = 1, 2, \ldots, n \quad (42)$$

The Galerkin approach

- Imposing the orthogonality condition and using the expression of the error one has

$$\mathrm{E}\left[\phi_j^T\left(\sum_{i=0}^{M}\mathbf{A}_i\xi_i(\theta)\right)\left(\sum_{k=1}^{n}c_k\widehat{\Gamma}_k(\boldsymbol{\xi}(\theta))\phi_k\right)-\phi_j^T\mathbf{f}\right]=0,\forall j \tag{43}$$

- Interchanging the $\mathrm{E}\left[\bullet\right]$ and summation operations, this can be simplified to

$$\sum_{k=1}^{n}\left(\sum_{i=0}^{M}\left(\phi_j^T\mathbf{A}_i\phi_k\right)\mathrm{E}\left[\xi_i(\theta)\widehat{\Gamma}_k(\boldsymbol{\xi}(\theta))\right]\right)c_k = \mathrm{E}\left[\phi_j^T\mathbf{f}\right] \tag{44}$$

$$\text{or}\quad \sum_{k=1}^{n}\left(\sum_{i=0}^{M}\widetilde{A}_{i_{jk}}D_{ijk}\right)c_k=b_j \tag{45}$$

Model Reduction by reduced number of basis

- Suppose the eigenvalues of $\mathbf{A}_0$ are arranged in an increasing order such that

$$\lambda_{0_1} < \lambda_{0_2} < \ldots < \lambda_{0_n} \tag{46}$$

- From the expression of the spectral functions observe that the eigenvalues ($\lambda_{0_k} = \omega_{0_k}^2$) appear in the denominator:

$$\Gamma_k^{(1)}(\omega, \boldsymbol{\xi}(\theta)) = \frac{\phi_k^T \mathbf{f}(\omega)}{\Lambda_{0_k}(\omega) + \sum_{i=1}^M \xi_i(\theta) \Lambda_{i_k}(\omega)} \tag{47}$$

where $\Lambda_{0_k}(\omega) = -\omega^2 + i\omega(\zeta_1 + \zeta_2 \omega_{0_k}^2) + \omega_{0_k}^2$

- The series can be truncated based on the magnitude of the eigenvalues relative to the frequency of excitation. Hence for the frequency domain analysis all the eigenvalues that cover almost twice the frequency range under consideration can be chosen.

Computational method

- The mean vector can be obtained as

$$\bar{\mathbf{u}} = \mathrm{E}\left[\hat{\mathbf{u}}(\theta)\right] = \sum_{k=1}^{p} c_k \mathrm{E}\left[\widehat{\Gamma}_k(\boldsymbol{\xi}(\theta))\right] \phi_k \tag{48}$$

- The covariance of the solution vector can be expressed as

$$\boldsymbol{\Sigma}_u = \mathrm{E}\left[\left(\hat{\mathbf{u}}(\theta) - \bar{\mathbf{u}}\right)\left(\hat{\mathbf{u}}(\theta) - \bar{\mathbf{u}}\right)^T\right] = \sum_{k=1}^{p}\sum_{j=1}^{p} c_k c_j \Sigma_{\Gamma_{kj}} \phi_k \phi_j^T \tag{49}$$

where the elements of the covariance matrix of the spectral functions are given by

$$\Sigma_{\Gamma_{kj}} = \mathrm{E}\left[\left(\widehat{\Gamma}_k(\boldsymbol{\xi}(\theta)) - \mathrm{E}\left[\widehat{\Gamma}_k(\boldsymbol{\xi}(\theta))\right]\right)\left(\widehat{\Gamma}_j(\boldsymbol{\xi}(\theta)) - \mathrm{E}\left[\widehat{\Gamma}_j(\boldsymbol{\xi}(\theta))\right]\right)\right] \tag{50}$$

Summary of the computational method

1. Solve the generalized eigenvalue problem associated with the mean mass and stiffness matrices to generate the orthonormal basis vectors: $\mathbf{K}_0\boldsymbol{\Phi} = \mathbf{M}_0\boldsymbol{\Phi}\boldsymbol{\lambda}_0$
2. Select a number of samples, say N_{samp}. Generate the samples of basic random variables $\xi_i(\theta), i = 1, 2, \ldots, M$.
3. Calculate the spectral basis functions (for example, first-order): $\Gamma_k\left(\omega, \boldsymbol{\xi}(\theta)\right) = \frac{\phi_k^T \mathbf{f}(\omega)}{\Lambda_{0_k}(\omega) + \sum_{i=1}^{M} \xi_i(\theta)\Lambda_{i_k}(\omega)}$, for $k = 1, \cdots p$, $p < n$
4. Obtain the coefficient vector: $\mathbf{c}(\omega) = \mathbf{S}^{-1}(\omega)\mathbf{b}(\omega) \in \mathbb{R}^n$, where $\mathbf{b}(\omega) = \widetilde{\mathbf{f}(\omega)} \odot \overline{\boldsymbol{\Gamma}(\omega)}$, $\mathbf{S}(\omega) = \boldsymbol{\Lambda}_0(\omega) \odot \mathbf{D}_0(\omega) + \sum_{i=1}^{M} \widetilde{\mathbf{A}}_i(\omega) \odot \mathbf{D}_i(\omega)$ and $\mathbf{D}_i(\omega) = \mathrm{E}\left[\boldsymbol{\Gamma}(\omega, \theta)\xi_i(\theta)\boldsymbol{\Gamma}^T(\omega, \theta)\right], \forall\, i = 0, 1, 2, \ldots, M$
5. Obtain the samples of the response from the spectral series: $\hat{\mathbf{u}}(\omega, \theta) = \sum_{k=1}^{p} c_k(\omega)\Gamma_k(\boldsymbol{\xi}(\omega, \theta))\phi_k$

The Euler-Bernoulli beam example

- An Euler-Bernoulli cantilever beam with stochastic bending modulus for a specified value of the correlation length and for different degrees of variability of the random field.

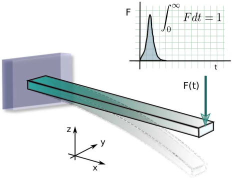

(c) Euler-Bernoulli beam

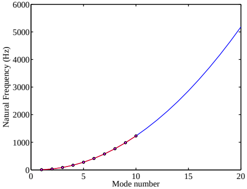

(d) Natural frequency distribution.

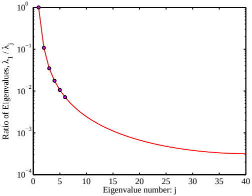

(e) Eigenvalue ratio of KL decomposition

- Length : 1.0 m, Cross-section : 39×5.93 mm^2, Young's Modulus: 2×10^{11} Pa.
- Load: Unit impulse at $t = 0$ on the free end of the beam.

Problem details

- The bending modulus $EI(x, \theta)$ of the cantilever beam is taken to be a homogeneous stationary lognormal random field of the form
- The covariance kernel associated with this random field is

$$C_a(x_1, x_2) = \sigma_a^2 e^{-(|x_1 - x_2|)/\mu_a} \tag{51}$$

  where μ_a is the correlation length and σ_a is the standard deviation.
- A correlation length of $\mu_a = L/5$ is considered in the present numerical study.

Problem details

The random field is assumed to be lognormal. The results are compared with the polynomial chaos expansion.

- The number of degrees of freedom of the system is n = 200.
- The K.L. expansion is truncated at a finite number of terms such that 90% variability is retained.
- direct MCS have been performed with 10,000 random samples and for three different values of standard deviation of the random field, $\sigma_a = 0.05, 0.1, 0.2$.
- Constant modal damping is taken with 1% damping factor for all modes.
- Time domain response of the free end of the beam is sought under the action of a unit impulse at $t = 0$
- Upto 4^{th} order spectral functions have been considered in the present problem. Comparison have been made with 4^{th} order Polynomial chaos results.

Mean of the response

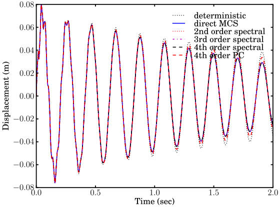

(f) Mean, $\sigma_a = 0.05$.

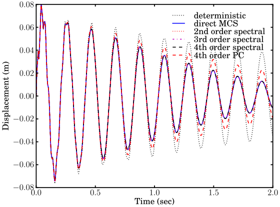

(g) Mean, $\sigma_a = 0.1$.

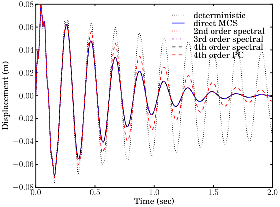

(h) Mean, $\sigma_a = 0.2$.

- Time domain response of the deflection of the tip of the cantilever for three values of standard deviation σ_a of the underlying random field.
- Spectral functions approach approximates the solution accurately.
- For long time-integration, the discrepancy of the 4^{th} order PC results increases.[3]

[3] Kundu, A., Adhikari, S., "Transient response of structural dynamic systems with parametric uncertainty", ASCE Journal of Engineering Mechanics, 140[2] (2014), pp. 315-331.

Standard deviation of the response

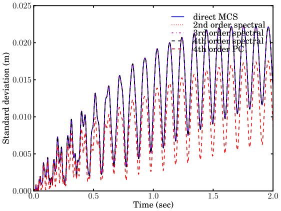

(i) Standard deviation of deflection, $\sigma_a = 0.05$.

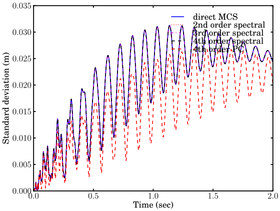

(j) Standard deviation of deflection, $\sigma_a = 0.1$.

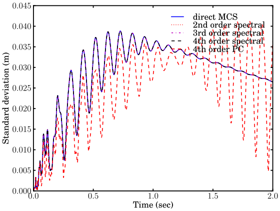

(k) Standard deviation of deflection, $\sigma_a = 0.2$.

- The standard deviation of the tip deflection of the beam.
- Since the standard deviation comprises of higher order products of the Hermite polynomials associated with the PC expansion, the higher order moments are less accurately replicated and tend to deviate more significantly.

Frequency domain response: mean

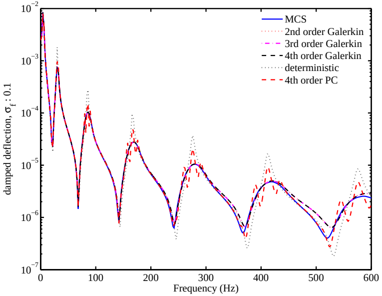

(l) Beam deflection for $\sigma_a = 0.1$.

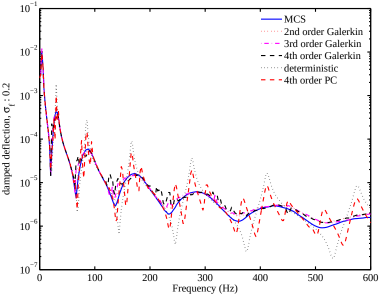

(m) Beam deflection for $\sigma_a = 0.2$.

[4] [5] The frequency domain response of the deflection of the tip of the Euler-Bernoulli beam under unit amplitude harmonic point load at the free end. The response is obtained with 10,000 sample MCS and for $\sigma_a = \{0.10, 0.20\}$.

[4] Jacquelin, E., Adhikari, S., Sinou, J.-J., and Friswell, M. I., "Polynomial chaos expansion and steady-state response of a class of random dynamical systems", ASCE Journal of Engineering Mechanics, 141[4] (2015), pp. 04014145:1-9.

[5] Jacquelin, E., Adhikari, S., Sinou, J.-J., and Friswell, M. I., "Polynomial chaos expansion in structural dynamics: Accelerating the convergence of the first two statistical moment sequences", Journal of Sound and Vibration, 356[11] (2015), pp. 144-154.

Frequency domain response: standard deviation

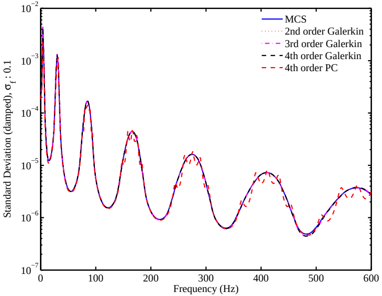

(n) Standard deviation of the response for $\sigma_a = 0.1$.

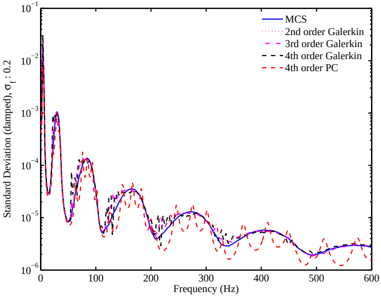

(o) Standard deviation of the response for $\sigma_a = 0.2$.

The standard deviation of the tip deflection of the Euler-Bernoulli beam under unit amplitude harmonic point load at the free end. The response is obtained with $10,000$ sample MCS and for $\sigma_a = \{0.10, 0.20\}$.

Experimental investigations

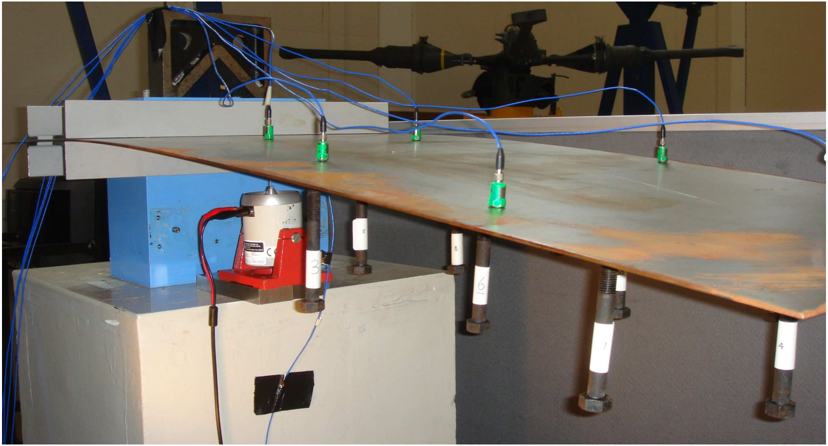

Figure: A cantilever plate with randomly attached oscillators[6]

[6] Adhikari, S., Friswell, M. I., Lonkar, K. and Sarkar, A., "Experimental case studies for uncertainty quantification in structural dynamics", Probabilistic Engineering Mechanics, 24[4] (2009), pp. 473-492.

Measured frequency response function

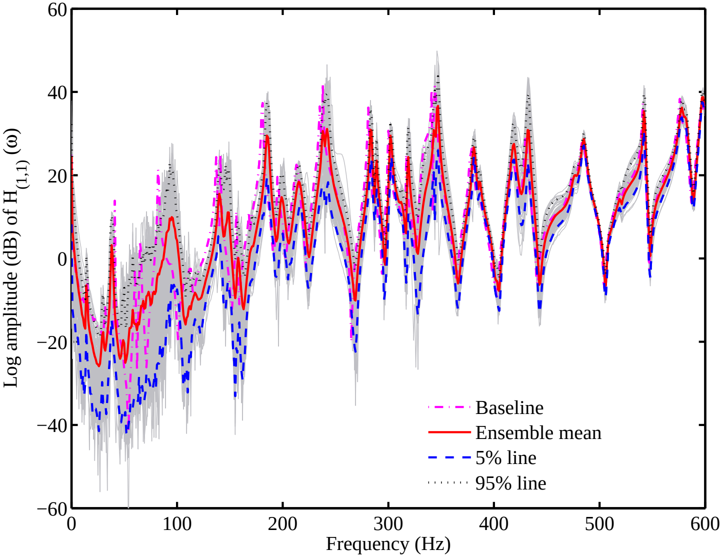

Piezoelectric vibration energy harvesting

- The harvesting of ambient vibration energy for use in powering low energy electronic devices has formed the focus of much recent research.
- Of the published results that focus on the piezoelectric effect as the transduction method, most have focused on harvesting using cantilever beams and on single frequency ambient energy, i.e., resonance based energy harvesting. Several authors have proposed methods to optimize the parameters of the system to maximize the harvested energy.
- Some authors have considered energy harvesting under wide band excitation.

Why uncertainty is important for energy harvesting?

- In the context of energy harvesting from ambient vibration, the input excitation may not be always known exactly.
- There may be uncertainties associated with the numerical values considered for various parameters of the harvester. This might arise, for example, due to the difference between the true values and the assumed values.
- If there are several nominally identical energy harvesters to be manufactured, there may be genuine parametric variability within the ensemble.
- Any deviations from the assumed excitation may result an optimally designed harvester to become sub-optimal.

Types of uncertainty

Suppose the set of coupled equations for energy harvesting:

$$\mathcal{L}\{\mathbf{u}(t)\} = \mathbf{f}(t) \tag{52}$$

Uncertainty in the input excitations

- For this case in general $\mathbf{f}(t)$ is a random function of time. Such functions are called random processes.
- $\mathbf{f}(t)$ can be Gaussian/non-Gaussian stationary or non-stationary random processes

Uncertainty in the system

- The operator $\mathcal{L}\{\bullet\}$ is in general a function of parameters $\theta_1, \theta_2, \cdots, \theta_n \in \mathbb{R}$.
- The uncertainty in the system can be characterised by the joint probability density function $p_{\Theta_1,\Theta_2,\cdots,\Theta_n}(\theta_1, \theta_2, \cdots, \theta_n)$.

Cantilever piezoelectric energy harvesters

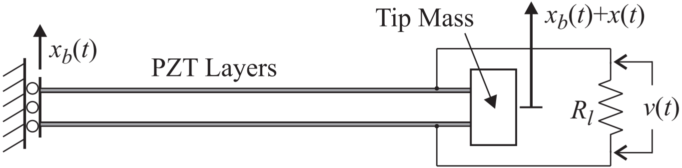

(a) Harvesting circuit without an inductor

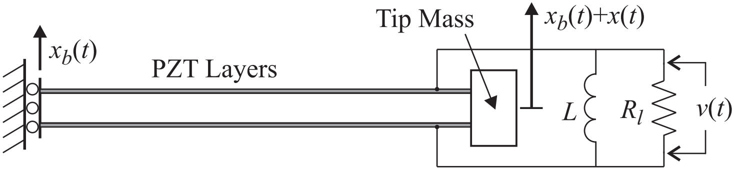

(b) Harvesting circuit with an inductor

Figure: Schematic diagrams of piezoelectric energy harvesters with two different harvesting circuits.

Governing equations

For the harvesting circuit without an inductor, the coupled electromechanical behavior can be expressed by the linear ordinary differential equations

$$m\ddot{x}(t) + c\dot{x}(t) + kx(t) - \theta v(t) = f(t) \tag{53}$$

$$\theta\dot{x}(t) + C_p\dot{v}(t) + \frac{1}{R_l}v(t) = 0 \tag{54}$$

For the harvesting circuit with an inductor, the electrical equation becomes

$$\theta\ddot{x}(t) + C_p\ddot{v}(t) + \frac{1}{R_l}\dot{v}(t) + \frac{1}{L}v(t) = 0 \tag{55}$$

Simplified piezomagnetoelastic model

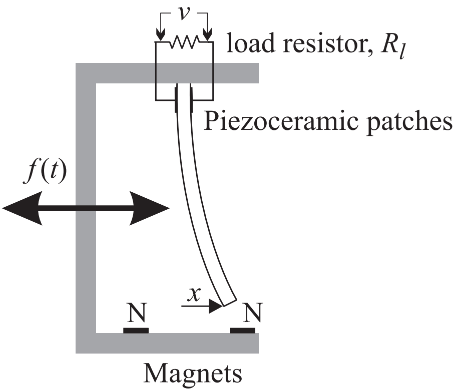

Schematic of the piezomagnetoelastic device. The beam system is also referred to as the 'Moon Beam'.

Governing equations

- The nondimensional equations of motion for this system are

$$\ddot{x} + 2\zeta\dot{x} - \frac{1}{2}x(1 - x^2) - \chi v = f(t), \tag{56}$$

$$\dot{v} + \lambda v + \kappa\dot{x} = 0, \tag{57}$$

- Here x is the dimensionless transverse displacement of the beam tip, v is the dimensionless voltage across the load resistor, χ is the dimensionless piezoelectric coupling term in the mechanical equation, κ is the dimensionless piezoelectric coupling term in the electrical equation, $\lambda \propto 1/R_l C_p$ is the reciprocal of the dimensionless time constant of the electrical circuit, R_l is the load resistance, and C_p is the capacitance of the piezoelectric material.
- The force $f(t)$ is proportional to the base acceleration on the device.
- If we consider the inductor, then the second equation will be $\ddot{v} + \lambda\dot{v} + \beta v + \kappa\ddot{x} = 0$.

Possible physically realistic cases

Depending on the system and the excitation, several cases are possible:

- Linear system excited by harmonic excitation
- Linear system excited by stochastic excitation
- Linear stochastic system excited by harmonic/stochastic excitation
- Nonlinear system excited by harmonic excitation
- Nonlinear system excited by stochastic excitation
- Nonlinear stochastic system excited by harmonic/stochastic excitation
- Multiple degree of freedom vibration energy harvesters

We focus on the application of random vibration theory to various energy harvesting problems

Circuit without an inductor

Our equations:

$$m\ddot{x}(t) + c\dot{x}(t) + kx(t) - \theta v(t) = -m\ddot{x}_b(t) \quad (58)$$

$$\theta\dot{x}(t) + C_p\dot{v}(t) + \frac{1}{R_l}v(t) = 0 \quad (59)$$

Transforming both the equations into the frequency domain and dividing the first equation by m and the second equation by C_p we obtain

$$\left(-\omega^2 + 2\mathrm{i}\omega\zeta\omega_n + \omega_n^2\right)X(\omega) - \frac{\theta}{m}V(\omega) = \omega^2 X_b(\omega) \quad (60)$$

$$\mathrm{i}\omega\frac{\theta}{C_p}X(\omega) + \left(\mathrm{i}\omega + \frac{1}{C_pR_l}\right)V(\omega) = 0 \quad (61)$$

Circuit without an inductor

The natural frequency of the harvester, ω_n, and the damping factor, ζ, are defined as

$$\omega_n = \sqrt{\frac{k}{m}} \quad \text{and} \quad \zeta = \frac{c}{2m\omega_n}. \tag{62}$$

Dividing the preceding equations by ω_n and writing in matrix form one has

$$\begin{bmatrix} (1-\Omega^2) + 2\mathrm{i}\Omega\zeta & -\frac{\theta}{k} \\ \mathrm{i}\Omega\frac{\alpha\theta}{C_p} & (\mathrm{i}\Omega\alpha + 1) \end{bmatrix} \begin{Bmatrix} X \\ V \end{Bmatrix} = \begin{Bmatrix} \Omega^2 X_b \\ 0 \end{Bmatrix}, \tag{63}$$

where the dimensionless frequency and dimensionless time constant are defined as

$$\Omega = \frac{\omega}{\omega_n} \quad \text{and} \quad \alpha = \omega_n C_p R_l. \tag{64}$$

α is the time constant of the first order electrical system, non-dimensionalized using the natural frequency of the mechanical system.

Circuit without an inductor

Inverting the coefficient matrix, the displacement and voltage in the frequency domain can be obtained as

$$\left\{ \begin{array}{c} X \\ V \end{array} \right\} = \frac{1}{\Delta_1} \begin{bmatrix} (\mathrm{i}\Omega\alpha+1) & \frac{\theta}{k} \\ -\mathrm{i}\Omega\frac{\alpha\theta}{C_p} & \left(1-\Omega^2\right)+2\mathrm{i}\Omega\zeta \end{bmatrix} \left\{ \begin{array}{c} \Omega^2 X_b \\ 0 \end{array} \right\} = \left\{ \begin{array}{c} (\mathrm{i}\Omega\alpha+1)\Omega^2 X_b/\Delta_1 \\ -\mathrm{i}\Omega^3\frac{\alpha\theta}{C_p} X_b/\Delta_1 \end{array} \right\}, \tag{65}$$

where the determinant of the coefficient matrix is

$$\Delta_1(\mathrm{i}\Omega) = (\mathrm{i}\Omega)^3\alpha + (2\,\zeta\,\alpha + 1)\,(\mathrm{i}\Omega)^2 + \left(\alpha + \kappa^2\alpha + 2\,\zeta\right)(\mathrm{i}\Omega) + 1 \tag{66}$$

and the non-dimensional electromechanical coupling coefficient is

$$\kappa^2 = \frac{\theta^2}{kC_p}. \tag{67}$$

Circuit without an inductor

Mean power

The average harvested power due to the white-noise base acceleration with a circuit without an inductor can be obtained as

$$\mathrm{E}\left[\widetilde{P}\right] = \mathrm{E}\left[\frac{|V|^2}{(R_l\omega^4\Phi_{x_bx_b})}\right]$$
$$= \frac{\pi\, m\,\alpha\,\kappa^2}{(2\,\zeta\,\alpha^2+\alpha)\,\kappa^2+4\,\zeta^2\alpha+(2\,\alpha^2+2)\,\zeta}.$$

- From Equation (65) we obtain the voltage in the frequency domain as

$$V = \frac{-\mathrm{i}\Omega^3\frac{\alpha\theta}{C_p}}{\Delta_1(\mathrm{i}\Omega)}X_b. \tag{68}$$

- We are interested in the mean of the normalized harvested power when the base acceleration is Gaussian white noise, that is $|V|^2/(R_l\omega^4\Phi_{x_bx_b})$.

Circuit without an inductor

The spectral density of the acceleration $\omega^4 \Phi_{x_b x_b}$ and is assumed to be constant. After some algebra, from Equation (68), the normalized power is

$$\widetilde{P} = \frac{|V|^2}{(R_l \omega^4 \Phi_{x_b x_b})} = \frac{k\alpha\kappa^2}{\omega_n^3} \frac{\Omega^2}{\Delta_1(\mathrm{i}\Omega)\Delta_1^*(\mathrm{i}\Omega)}. \tag{69}$$

Using linear stationary random vibration theory, the average normalized power can be obtained as

$$\mathrm{E}\left[\widetilde{P}\right] = \mathrm{E}\left[\frac{|V|^2}{(R_l \omega^4 \Phi_{x_b x_b})}\right] = \frac{k\alpha\kappa^2}{\omega_n^3} \int_{-\infty}^{\infty} \frac{\Omega^2}{\Delta_1(\mathrm{i}\Omega)\Delta_1^*(\mathrm{i}\Omega)} \mathrm{d}\omega \tag{70}$$

From Equation (66) observe that $\Delta_1(\mathrm{i}\Omega)$ is a third order polynomial in $(\mathrm{i}\Omega)$. Noting that $\mathrm{d}\omega = \omega_n \mathrm{d}\Omega$ and from Equation (66), the average harvested power can be obtained from Equation (70) as

$$\mathrm{E}\left[\widetilde{P}\right] = \mathrm{E}\left[\frac{|V|^2}{(R_l \omega^4 \Phi_{x_b x_b})}\right] = m\alpha\kappa^2 I^{(1)} \tag{71}$$

Circuit without an inductor

$$I^{(1)} = \int_{-\infty}^{\infty} \frac{\Omega^2}{\Delta_1(\mathrm{i}\Omega)\Delta_1^*(\mathrm{i}\Omega)}\,\mathrm{d}\Omega. \tag{72}$$

After some algebra, this integral can be evaluated as

$$I^{(1)} = \frac{\pi}{\alpha} \frac{\det\begin{bmatrix} 0 & 1 & 0 \\ -\alpha & \alpha+\kappa^2\alpha+2\,\zeta & 0 \\ 0 & -2\,\zeta\,\alpha-1 & 1 \end{bmatrix}}{\det\begin{bmatrix} 2\,\zeta\,\alpha+1 & -1 & 0 \\ -\alpha & \alpha+\kappa^2\alpha+2\,\zeta & 0 \\ 0 & -2\,\zeta\,\alpha-1 & 1 \end{bmatrix}} \tag{73}$$

Combining this with Equation (71) we obtain the average harvested power due to white-noise base acceleration.

Normalised mean power: numerical illustration

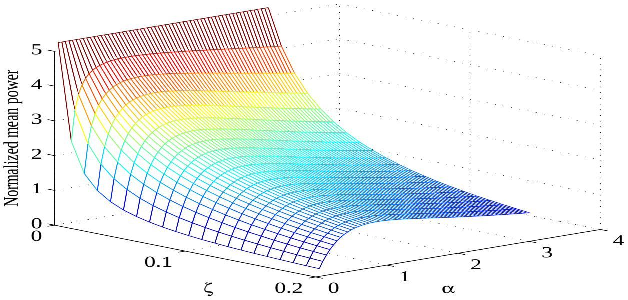

The normalized mean power of a harvester without an inductor as a function of α and ζ, with $\kappa = 0.6$. Maximizing the average power with respect to α gives the condition $\alpha^2 \left(1 + \kappa^2\right) = 1$ or in terms of physical quantities

$$R_l^2 C_p \left(kC_p + \theta^2\right) = m.$$

Circuit with an inductor

The electrical equation becomes

$$\theta\ddot{x}(t) + C_p\ddot{v}(t) + \frac{1}{R_l}\dot{v}(t) + \frac{1}{L}v(t) = 0 \tag{74}$$

where L is the inductance of the circuit. Transforming equation (74) into the frequency domain and dividing by $C_p\omega_n^2$ one has

$$-\Omega^2\frac{\theta}{C_p}X + \left(-\Omega^2 + \mathrm{i}\Omega\frac{1}{\alpha} + \frac{1}{\beta}\right)V = 0 \tag{75}$$

where the second dimensionless constant is defined as

$$\beta = \omega_n^2 L C_p, \tag{76}$$

Two equations can be written in a matrix form as

$$\begin{bmatrix} \left(1-\Omega^2\right)+2\mathrm{i}\Omega\zeta & -\frac{\theta}{k} \\ -\Omega^2\frac{\alpha\beta\theta}{C_p} & \alpha\left(1-\beta\Omega^2\right)+\mathrm{i}\Omega\beta \end{bmatrix}\left\{\begin{matrix} X \\ V \end{matrix}\right\} = \left\{\begin{matrix} \Omega^2 X_b \\ 0 \end{matrix}\right\}. \tag{77}$$

Circuit with an inductor

Inverting the coefficient matrix, the displacement and voltage in the frequency domain can be obtained as

$$
\left\{ \begin{array}{c} X \\ V \end{array} \right\} = \frac{1}{\Delta_2} \begin{bmatrix} \alpha\left(1-\beta\Omega^2\right)+\mathrm{i}\Omega\beta & \frac{\theta}{k} \\ \Omega^2 \frac{\alpha\beta\theta}{C_p} & \left(1-\Omega^2\right)+2\mathrm{i}\Omega\zeta \end{bmatrix} \left\{ \begin{array}{c} \Omega^2 X_b \\ 0 \end{array} \right\}
= \left\{ \begin{array}{c} \left(\alpha\left(1-\beta\Omega^2\right)+\mathrm{i}\Omega\beta\right)\Omega^2 X_b/\Delta_2 \\ \Omega^4 \frac{\alpha\beta\theta}{C_p} X_b/\Delta_2 \end{array} \right\} \tag{78}
$$

where the determinant of the coefficient matrix is

$$
\Delta_2(\mathrm{i}\Omega) = (\mathrm{i}\Omega)^4 \beta\,\alpha + (2\,\zeta\,\beta\,\alpha + \beta)\,(\mathrm{i}\Omega)^3 + \left(\beta\,\alpha + \alpha + 2\,\zeta\,\beta + \kappa^2 \beta\,\alpha\right)(\mathrm{i}\Omega)^2 + (\beta + 2\,\zeta\,\alpha)\,(\mathrm{i}\Omega) + \alpha. \tag{79}
$$

Circuit with an inductor

Mean power

The average harvested power due to the white-noise base acceleration with a circuit with an inductor can be obtained as

$$\mathrm{E}\left[\widetilde{P}\right] = \frac{m\alpha\beta\kappa^2\pi\left(\beta + 2\alpha\zeta\right)}{\beta\left(\beta + 2\alpha\zeta\right)\left(1 + 2\alpha\zeta\right)\left(\alpha\kappa^2 + 2\zeta\right) + 2\alpha^2\zeta\left(\beta - 1\right)^2}.$$

- We can determine optimum values for α and β. Dividing both the numerator and denominator of the above expression by $\beta\left(\beta + 2\alpha\zeta\right)$ shows that the optimum value of β for all values of the other parameters is $\beta = 1$. This value of β implies that $\omega_n^2 L C_p = 1$, and thus the mechanical and electrical natural frequencies are equal.
- With $\beta = 1$ the average normalized harvested power is

$$\mathrm{E}\left[\widetilde{P}\right] = \frac{m\alpha\kappa^2\pi}{\left(1 + 2\alpha\zeta\right)\left(\alpha\kappa^2 + 2\zeta\right)}. \tag{80}$$

If κ and ζ are fixed then the maximum power with respect to α is obtained when $\alpha = 1/\kappa$.

Normalised mean power: numerical illustration

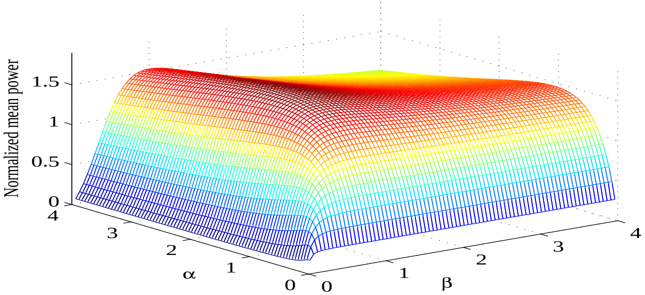

The normalized mean power of a harvester with an inductor as a function of α and β, with $\zeta = 0.1$ and $\kappa = 0.6$.

Optimal parameter selection

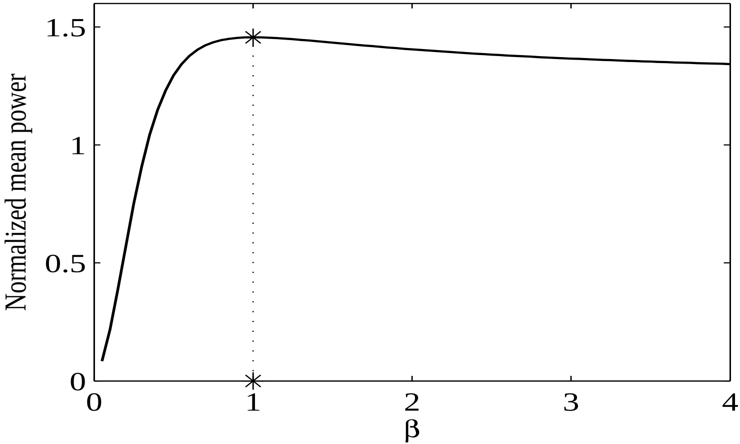

The normalized mean power of a harvester with an inductor as a function of β for $\alpha = 0.6$, $\zeta = 0.1$ and $\kappa = 0.6$. The * corresponds to the optimal value of $\beta (= 1)$ for the maximum mean harvested power.

Optimal parameter selection

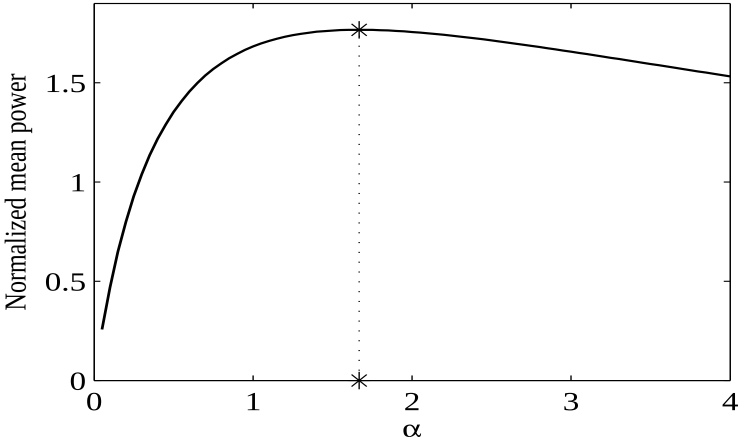

The normalized mean power of a harvester with an inductor as a function of α for $\beta = 1$, $\zeta = 0.1$ and $\kappa = 0.6$. The * corresponds to the optimal value of $\alpha (= 1.667)$ for the maximum mean harvested power.

Nonlinear coupled equations

$$\ddot{x} + 2\zeta\dot{x} + g(x) - \chi v = f(t) \tag{81}$$

$$\dot{v} + \lambda v + \kappa\dot{x} = 0, \tag{82}$$

The nonlinear stiffness is represented as $g(x) = -\frac{1}{2}(x - x^3)$. Assuming a non-zero mean random excitation (i.e., $f(t) = f_0(t) + m_f$) and a non-zero mean system response (i.e., $x(t) = x_0(t) + m_x$), the following equivalent linear system is considered,

$$\ddot{x}_0 + 2\zeta\dot{x}_0 + a_0 x_0 + b_0 - \chi v = f_0(t) + m_f \tag{83}$$

where $f_0(t)$ and $x_0(t)$ are zero mean random processes. m_f and m_x are the mean of the original processes $f(t)$ and $x(t)$ respectively. a_0 and b_0 are the constants to be determined with $b_0 = m_f$ and a_0 represents the square of the natural frequency of the linearized system ω_{eq}^2.

Linearised equations

We minimise the expectation of the error norm i.e., $(\mathbb{E}\left[\epsilon^2\right], \text{with } \epsilon = g(x) - a_0 x_0 - b_0)$. To determine the constants a_0 and b_0 in terms of the statistics of the response x, we take partial derivatives of the error norm *w.r.t.* a_0 and b_0 and equate them to zero individually.

$$\frac{\partial}{\partial a_0}\mathrm{E}\left[\epsilon^2\right] = \mathrm{E}\left[g(x)x_0\right] - a_0\mathrm{E}\left[x_0^2\right] - b_0\mathrm{E}\left[x_0\right] \tag{84}$$

$$\frac{\partial}{\partial b_0}\mathrm{E}\left[\epsilon^2\right] = \mathrm{E}\left[g(x)\right] - a_0\mathrm{E}\left[x_0\right] - b_0 \tag{85}$$

Equating (84) and (85) to zero, we get,

$$a_0 = \frac{\mathrm{E}\left[g(x)x_0\right]}{\mathrm{E}\left[x_0^2\right]} = \frac{\mathrm{E}\left[g(x)x_0\right]}{\sigma_x^2} \tag{86}$$

$$b_0 = \mathrm{E}\left[g(x)\right] = m_f \tag{87}$$

Responses of the piezomagnetoelastic oscillator

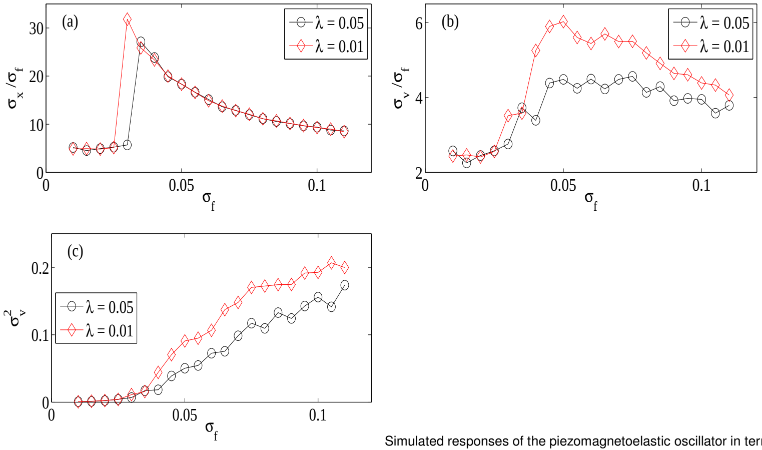

Simulated responses of the piezomagnetoelastic oscillator in terms of the standard deviations of displacement and voltage (σ_X and σ_V) as the standard deviation of the random excitation σ_f varies. (a) gives the ratio of the displacement and excitation; (b) gives the ratio of the voltage and excitation; and (c) shows the variance of the voltage, which is proportional to the mean power.

Phase portraits

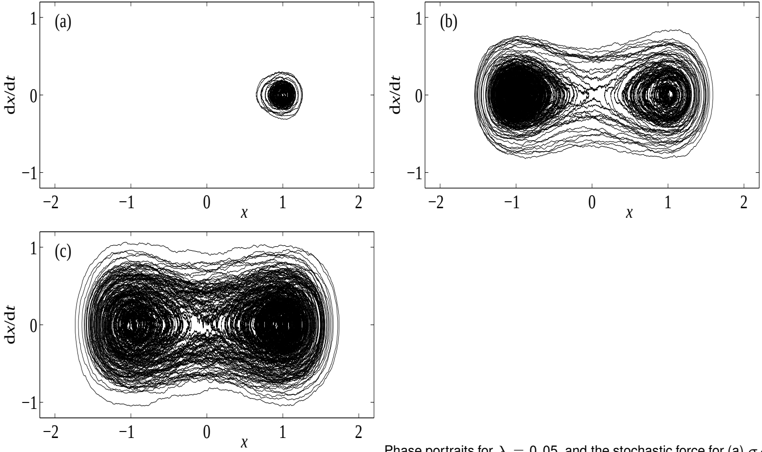

Phase portraits for $\lambda = 0.05$, and the stochastic force for (a) $\sigma_f = 0.025$, (b) $\sigma_f = 0.045$, (c) $\sigma_f = 0.065$. Note that the increasing noise level overcomes the potential barrier resulting in a significant increase in the displacement x.

Voltage output

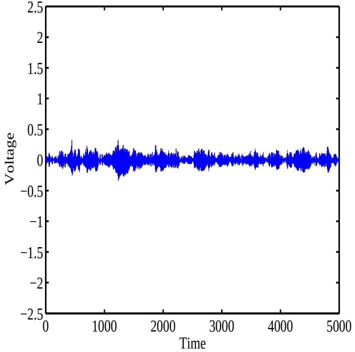

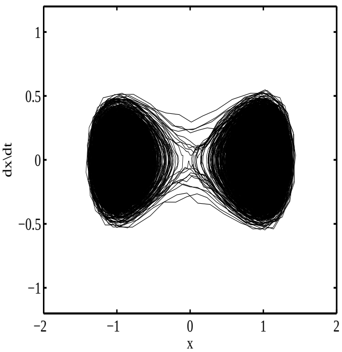

Voltage output due to Gaussian white noise ($\zeta = 0.01$, $\chi = 0.05$, and $\kappa = 0.5$ and $\lambda = 0.01$.

Voltage output

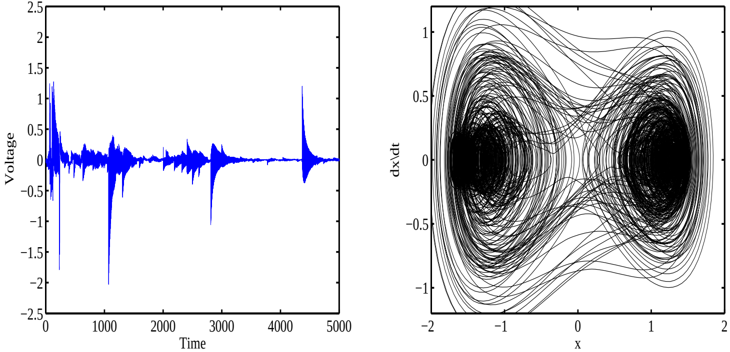

Voltage output due to Lévy noise ($\zeta = 0.01$, $\chi = 0.05$, and $\kappa = 0.5$ and $\lambda = 0.01$.

Inverted beam harvester

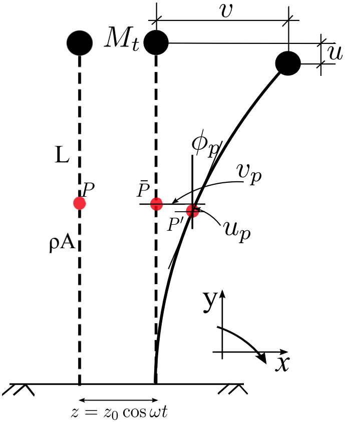

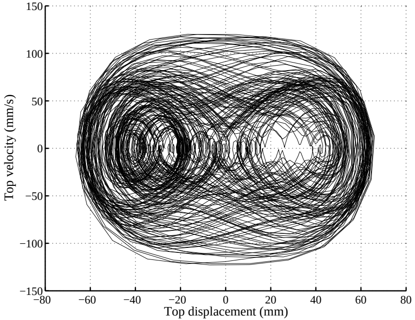

(a) Schematic diagram of inverted beam harvester, (b) a typical phase portrait of the tip mass.

Fokker-Planck (FP) equation analysis for nonlinear EH

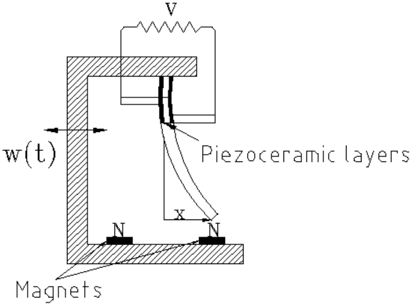

$$\ddot{X} + c\dot{X} + k(-X + \alpha X^3) - \chi V = \sigma W(t), \tag{88}$$

$$\dot{V} + \lambda V + \beta \dot{X} = 0 \tag{89}$$

$W(t)$ is a stationary, zero mean unit Gaussian white noise process with $E[W(t)W(t+\tau)] = \delta(\tau)$, σ is the intensity of excitation. The two sided power spectral density of the white noise excitation on the RHS of Eq. (88) corresponding to this intensity is $\sigma^2/2\pi$.

State-space form

- Eqs. (88) and (89) can be expressed in state space form by introducing the variables $X_1 = X$, $X_2 = \dot{X}$ and $X_3 = V$, as

$$\left\{ \begin{array}{c} \mathrm{d}X_1(t) \\ \mathrm{d}X_2(t) \\ \mathrm{d}X_3(t) \end{array} \right\} = \left\{ \begin{array}{c} X_2 \\ k(X_1 - \alpha X_1^3) - cX_2 + \chi X_3 \\ -\beta X_2 - \lambda X_3 \end{array} \right\} \mathrm{d}t + \left\{ \begin{array}{c} 0 \\ \sigma \\ 0 \end{array} \right\} \mathrm{d}B(t). \tag{90}$$

  where $B(t)$ is the unit Wiener process.

- The FP equation can be derived from the Itô SDE of the form

$$\mathrm{d}\mathbf{X}(t) = \mathbf{m}[\mathbf{X}, t]\mathrm{d}t + \mathbf{h}[\mathbf{X}, t]\mathrm{d}\mathbf{B}, \tag{91}$$

  where $B(t)$ is the normalized Wiener process and the corresponding FP equation of $\mathbf{X}(t)$ is given by

$$\frac{\partial p(\mathbf{X}, t|\mathbf{X}^0, t_0)}{\partial t} = \Big[-\sum_{i=1}^{N} \frac{\partial [m_i(\mathbf{X}, t)]}{\partial X_i} + \frac{1}{2} \sum_{i=1}^{N} \sum_{j=1}^{N} \frac{\partial^2 [h_{ij}(\mathbf{X}, t)]}{\partial X_i \partial X_j} \Big] p(\mathbf{X}, t|\mathbf{X}^0, t_0) \tag{92}$$

  where $p(\mathbf{X}, t)$ is the joint PDF of the N-dimensional system state $\mathbf{X}$

FP equation for nonlinear stochastic EH problems

- Eqs. (90) of the energy harvesting system are of the form of the SDE (91) and the corresponding FP equation can be expressed as per Eq. (92) as

$$\begin{aligned}\frac{\partial p}{\partial t} = -X_2\frac{\partial p}{\partial X_1} + (cX_2 - k(X_1 + \alpha X_1^3) - \chi X_3)\frac{\partial p}{\partial X_2} + \\ (\beta X_2 + \lambda X_3)\frac{\partial p}{\partial X_3} + \frac{\sigma^2}{2}\frac{\partial^2 p}{\partial X_2^2} + (c+\lambda)p\end{aligned} \tag{93}$$

  where $p = p(\mathbf{X}, t|\mathbf{X}^0, t_0)$ the joint transition PDF of the state variables is used for notational convenience satisfying the conditions

$$\int_{-\infty}^{\infty} p(\mathbf{X}, t|\mathbf{X}^0, t_0)\,\mathrm{d}\mathbf{X} = 1, \quad \lim_{t\to 0} p(\mathbf{X}, t|\mathbf{X}^0, t_0) = \delta(\mathbf{X}-\mathbf{X}^0), \tag{94}$$

$$p(\mathbf{X}, t|\mathbf{X}^0, t_0)|_{X_i\to\pm\infty} = 0, \quad (i = 1, \ldots, n). \tag{95}$$

- A finite element (FE) based method is developed for the solution of the FP equation.

FEM for FP equations

- The weak form of the FP equation can be obtained as

$$\mathbf{M}\dot{\mathbf{p}} + \mathbf{K}\mathbf{p} = \mathbf{0}, \tag{96}$$

subject to the initial condition $\mathbf{p}(0) = \mathbf{p}$, where, $\mathbf{p}$ is a vector of the joint PDF at the nodal points.

$$\mathbf{M} = [< \psi_r, \psi_s >]_\Omega, \tag{97}$$

$$\mathbf{K} = \int_\Omega \Big[\sum_{i=1}^{N} \psi_r(\mathbf{X}) \frac{\partial[m_i(\mathbf{X})\psi_s(\mathbf{X})]}{\partial X_j} \Big] \mathrm{d}\mathbf{X} + \int_\Omega \Big[\sum_{i=1}^{N} \sum_{j=1}^{N} \frac{\partial[\psi_r(\mathbf{X})]}{\partial X_i} \frac{\partial[h_{ij}\psi_s(\mathbf{X})]}{\partial X_j} \mathrm{d}\mathbf{X} \Big]. \tag{98}$$

- A solution of Eq. (96) is obtained using the Crank-Nicholson method, which is an implicit time integration scheme with second order accuracy and unconditional stability:

$$[\mathbf{M} - \Delta t(1-\theta)\mathbf{K}]\mathbf{p}(t+\Delta t) = [\mathbf{M} + \Delta t\theta\mathbf{K}]\mathbf{p}(t). \tag{99}$$

The parameter $\theta = 0.5$ and Δt is the time step.

Joint PDF of the response

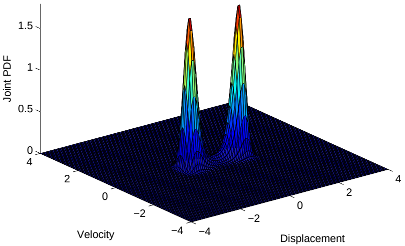

(a) Response PDF

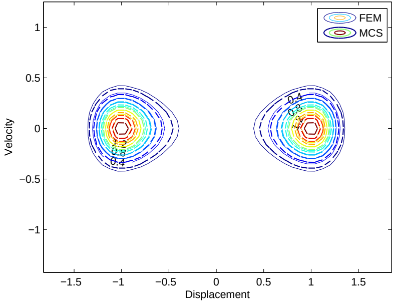

(b) Contour plot comparison

Figure: Joint PDF and contour plots of piezomagnetoelastic Energy Harvester ($c = 0.02, \lambda = 0.01, \sigma = 0.04$)

Joint PDF of the response

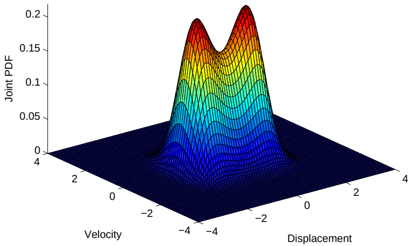

(a) Response PDF

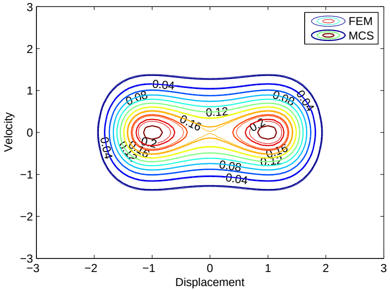

(b) Contour plot comparison

Figure: Joint PDF and contour plots of piezomagnetoelastic Energy Harvester ($c = 0.02, \lambda = 0.01, \sigma = 0.12$)

Conclusions

- The mean response of a damped stochastic system is more damped than the underlying baseline system
- For small damping, $\xi_e \approx \frac{3^{1/4}\sqrt{\epsilon}}{\sqrt{\pi}}\sqrt{\xi}$
- Conventional response surface based methods fails to capture the physics of damped dynamic systems
- Proposed spectral function approach uses the undamped modal basis and can capture the statistical trend of the dynamic response of stochastic damped MDOF systems
- The solution is projected into the modal basis and the associated stochastic coefficient functions are obtained at each frequency step (or time step).
- The coefficient functions, called as the spectral functions, are expressed in terms of the spectral properties (natural frequencies and mode shapes) of the system matrices.
- The proposed method takes advantage of the fact that for a given maximum frequency only a small number of modes are necessary to represent the dynamic response. This modal reduction leads to a significantly smaller basis.

Conclusions

- Vibration energy based piezoelectric and magnetopiezoelectric energy harvesters are expected to operate under a wide range of ambient environments. This talk considers energy harvesting of such systems under harmonic and random excitations.
- Optimal design parameters were obtained using the theory of linear random vibration
- Nonlinearity of the system can be exploited to scavenge more energy over wider operating conditions
- The Fokker-Planck equation corresponding to the nonlinear piezomagnetoe- lastic energy harvester excited by Gaussian white noise was derived and solved using the finite element method

Further details

1. http://engweb.swan.ac.uk/∼adhikaris/renewable_energy.html
2. Litak, G., Friswell, M. I. and Adhikari, S., "Regular and chaotic vibration in a piezoelectric energy harvester", Meccanica, in press.
3. Madinei, H., Khodaparast, H. H., Adhikari, S. Friswell, M. I., Fazeli, M., "An adaptively tuned piezoelectric MEMS vibration energy harvester using an electrostatic device", European Physical Journal Special Topics (EPJ-ST), 224[14] (2015), pp. 2703-2717.
4. Friswell, M. I., Bilgen, O., Ali, S. F., Litak, G. and Adhikari, S., "The effect of noise on the response of a vertical cantilever beam energy harvester", Zeitschrift fur Angewandte Mathematik und Mechanik (ZAMM), 95[5] (2015), pp. 433-443.
5. Borowiec, B., Litak, G., Friswell, M. I. and Adhikari, S., "Energy harvesting in a nonlinear cantilever piezoelastic beam system excited by random vertical vibrations", International Journal of Structural Stability and Dynamics, 14[8] (2014), pp. 1440018:1-13.
6. Kumar, P., Narayanan, S., Adhikari, S. and Friswell, M. I., "Fokker-Planck equation analysis of randomly excited nonlinear energy harvester", Journal of Sound and Vibration, 333[7] (2014), pp. 2040-2053.
7. Borowiec, B., Litak, G., Friswell, M. I., Ali, S. F., Adhikari, S. and Lees, A. W. and Bilgen, O., "Energy harvesting in piezoelastic systems driven by random excitations", International Journal of Structural Stability and Dynamics, 13[7] (2013), pp. 1340006:1-11
8. Ali, S. F. and Adhikari, S., "Energy harvesting dynamic vibration absorbers", Transactions of ASME, Journal of Applied Mechanics.
9. Friswell, M. I., Ali, S. F., Adhikari, S., Lees, A.W. , Bilgen, O. and Litak, G., "Nonlinear piezoelectric vibration energy harvesting from an inverted cantilever beam with tip mass", Journal of Intelligent Material Systems and Structures, 23[3] (2012), pp. 1505-1521.
10. Litak, G., Friswell, M. I., Kitio Kwuimy, C. A., Adhikari, S. and Borowiec, B., "Energy harvesting by two magnetopiezoelastic oscillators with mistuning", Theoretical & Applied Mechanics Letters, 2[4] (2012), pp. 043009.
11. Ali, S. F., Friswell, M. I. and Adhikari, S., "Analysis of energy harvesters for highway bridges", Journal of Intelligent Material Systems and Structures, 22[16] (2011), pp. 1929-1938.

Further details

12. Jacquelin, E., Adhikari, S. and Friswell, M. I., ”Piezoelectric device for impact energy harvesting”, Smart Materials and Structures, 20[10] (2011), pp. 105008:1-12.
13. Litak, G., Borowiec, B., Friswell, M. I. and Adhikari, S., ”Energy harvesting in a magnetopiezoelastic system driven by random excitations with uniform and Gaussian distributions”, Journal of Theoretical and Applied Mechanics, 49[3] (2011), pp. 757-764..
14. Ali, S. F., Adhikari, S., Friswell, M. I. and Narayanan, S., ”The analysis of piezomagnetoelastic energy harvesters under broadband random excitations”, Journal of Applied Physics, 109[7] (2011), pp. 074904:1-8
15. Ali, S. F., Friswell, M. I. and Adhikari, S., ”Piezoelectric energy harvesting with parametric uncertainty”, Smart Materials and Structures, 19[10] (2010), pp. 105010:1-9.
16. Friswell, M. I. and Adhikari, S., ”Sensor shape design for piezoelectric cantilever beams to harvest vibration energy”, Journal of Applied Physics, 108[1] (2010), pp. 014901:1-6.
17. Litak, G., Friswell, M. I. and Adhikari, S., ”Magnetopiezoelastic energy harvesting driven by random excitations”, Applied Physics Letters, 96[5] (2010), pp. 214103:1-3.
18. Adhikari, S., Friswell, M. I. and Inman, D. J., ”Piezoelectric energy harvesting from broadband random vibrations”, Smart Materials and Structures, 18[11] (2009), pp. 115005:1-7.

Future works / possible collaborations

- Coupled fluid-structure-piezo systems with parametric uncertainties - enhancing the spectral function method
- Reduced model approach for stochastically parameter coupled fluid-structure-piezo systems
- Quantification of harvested energy for general piezo systems with random excitations